https://doi.org/10.33271/nvngu/2024-2/074

V. H. Puzyr,
orcid.org/0000-0001-6096-9049,
S. V. Mykhalkiv*,
orcid.org/0000-0002-0425-6295,
O. A. Plakhtii,
orcid.org/0000-0002-1535-8991

Ukrainian State University of Railway Transport, Kharkiv, Ukraine
* Corresponding author e-mail: svm_m@kart.edu.ua

A HYBRID ICEEMDAN AND OMEDA-BASED VIBRODIAGNOSIS METHOD FOR THE BEARING OF ROLLING STOCK

Purpose. To develop a hybrid method based on ICEEMDAN and OMEDA for high-fidelity detection of the diagnostic features of the technical condition of roller bearing.

Methodology. Due to digital signal processing the search was made of the informative components on the broadband spectra, envelope spectra, squared envelope spectra. The usage of the methods of mathematical statistics for the selection of informative IMFs as a result of iterative calculate procedures. The introduction of blind deconvolution method with a proper objective function for the enhancement of impulse fault features.

Findings. The use of traditional spectral methods provided an incomplete list of diagnostic features of bearing roller damage. The empirical mode decomposition (EMD) method and its minor versions provide the series of intrinsic mode functions (IMFs). On the broadband vibration spectra of the selected low-frequency IMFs, diagnostic features were not detected in a sufficient number. Further research focused on the development of a hybrid method that takes into account the demodulation procedure of the high-frequency components of those IMFs that were selected according to the complex evaluation index. The Fast Kurtogram technique determined an informative frequency band of 7.2–7.5 kHz for demodulation and construction of the squared envelope spectra, where harmonics of the roller spin frequency and some side bands with a width equal to the separator rotation frequency appeared. The use of OMEDA caused the reduction of residual noise on the squared envelope spectra and bilateral sidebands to appear around all harmonics of the roller spin frequency.

Originality. For the first time, the whole list of the diagnostic features of roller faults of the axle-box bearing was identified using the developed hybrid method, which involves steps of noise reduction for enhancing a physical meaning of a proper frequency components, associated with faults. The usage of the optimal minimum entropy deconvolution adjusted method helped to eliminate noise and provide all diagnostic features of the technical condition on the squared envelope spectrum.

Practical value. The results of the study help to control the quality of repair of the axle-box rolling bearings on the test rig at the workshop of the freight railway car depot.

Keywords: *car, vibration, diagnostics, bearing, deconvolution, decomposition, spectrum*

Introduction. Rolling bearings are the most common components for all types of equipment with rotating elements in various industries. According to statistics, 30 % equipment failures are associated with bearing failures [1]. In the mining industry, the implementation of a real-time condition monitoring system for critical components with rolling bearings and gears of grinding mills, which consume more than 50 % of the mining factory's energy, is becoming increasingly important [2]. In the railway industry, the health of the rolling bearings of axle-boxes directly affects the safety of the operation. Therefore, the introduction of vibrodiagnostic methods for fault detection in rolling bearings is crucial, since only 10–20 % axle-box bearings, according to statistical data, can reach the designed life longevity [3]. However, information for most faults cannot be obtained from visual observation of signals alone, due to their random behavior and the processes that generate them. Therefore, researchers currently focus on developing new diagnostic tools and techniques in accordance with the features of a particular equipment, or on adjusting classical tools to obtain the appropriate result in particular cases [1].

Literature review. Typically, the vibration of rolling bearings is non-stationary and nonlinear and filled with noise. However, the impulses caused by faults are in practice too weak to be distinguished from the signal, which is filled with strong noise, using traditional techniques, such as kurtosis and envelope spectrum [4]. Therefore, signal enhancement techniques are used, such as filtering (classical, adaptive, and optimal filters), simulation (cyclostationary, stochastic), or wavelet decomposition [5]. Unfortunately, over the years, wavelet analysis has demonstrated disadvantages, such as the dependence of accuracy on the choice of the basis wavelet function [6]. Also, the lack of adaptability in the wavelet decomposition leads a priori to a subjective assumption about the characteristics of the vibration signal being studied. As a result, only those signal characteristics that correlate with the shape of the basis wavelet function can affect the significance of the coefficients based on the calculation results. Other characteristics will be either hidden or completely ignored [7]. In addition, wavelet decomposition cannot accurately separate the high-frequency band, where information about the existing fault is always located [4].

The empirical mode decomposition (EMD) is adaptive and can decompose non-stationary signals into a number of intrinsic mode functions (IMFs) and introduce a more realistic representation of the signal free from artefacts introduced by non-adaptive Fourier transform constraints and wavelet analysis. However, EMD has many drawbacks, such as excessive decomposition and the mode mixing effect [4, 8].

Additional consideration was given to the selection of informative IMFs obtained as a result of implementation of the EMD and its optimized versions. The sensitive IMF was selected by evaluating the similarity. Also, the maximum kurtosis criterion or the calculation of mutual information between IMFs and the original signal with a fault was proposed to identify those modes where a fault is manifested and which have the appropriate sensitivity [9].

To make self-adaptive techniques more effective, they are usually combined with other methods. In [10], a hybrid method based on a combination of EEMD and spectral kurtosis is proposed to distinguish features of bearing faults from strong noise. In [11], minimum entropy deconvolution (MED) is combined with EMD and the Teager-Kaiser energy operator to demodulate acoustic and vibration signals for bearing fault diagnosis. In [12], EMD was used to diagnose rolling bearings after a noise reduction using wavelet transform. The authors

of [13] found that the proposed hybrid method, consisting of a combination of EMD and wavelet multiresolution analysis, provides more effective damage detection than each of the above approaches separately.

Unsolved aspects of the problem. Despite the obvious successes in distinguishing informative IMFs based on the results of EMD and its minor versions, the existing residual noise obviously prevents from obtaining the bearing frequency components from the selected IMF by implementing the traditional FFT algorithm [4, 14]. The results of the separate application of the other mentioned techniques are also characterized by insufficient enhancement of the useful components on the broadband and envelope vibration spectra.

Therefore, the development of hybrid methods that combine the effectiveness of self-adaptive methods with the properties of tools for amplifying the impulse components of vibration allows solving the problem of diagnosing faults of rolling bearings in the corresponding units.

Purpose. The purpose of the article is to develop a hybrid method based on ICEEMDAN and a deconvolution method, which involves D-norm as an objective function.

The following problems should be solved to achieve the above purpose:

- acceptability of traditional spectral techniques to distinguish diagnostic features of faults of the rolling bearing elements;
- selecting an approach to opting for informative IMF based on the results of decomposition by the EMD and its versions;
- determination of the effectiveness of the EMD and its versions in the decomposition of the studied vibration signal;
- substantiation of the need for further deconvolution of the selected IMF in order to increase the number of diagnostic features of the technical condition and eliminate the residual noise.

Methods. To develop a hybrid method of vibrodiagnosis, first digital signal processing in the time and frequency dimensions were studied to determine their ability to detect features of faults of a bearing roller at an early stage of development. Further, the EMD and its later versions were used to decompose the signal under study into sets of IMFs, followed by the selection of the IMFs whose energy bursts cover the frequency band that includes the rotating frequencies of the rolling bearing elements. After determining the informative IMF using statistical indicators, the fast kurtogram was used to determine the frequency band with the highest energy burst for further demodulation and acquiring squared envelope spectra. Finally, the expediency of using the blind decomposition to obtain additional diagnostic features on the squared envelope spectra was determined.

Results. During the experimental studies, an axle-box rolling bearing 30-232726 E2M with a roller, which had a smearing damage on its cylindrical surface was installed on the test rig (Fig. 1).

The inner race of the bearing was rotated to the rotation frequency $n = 735$ rpm. After the analog low-pass filter with the cutoff frequency 9 kHz, the signal acquired by the vibration accelerometer discretized in the analog-to-digital converter with the period of $2.17 \cdot 10^{-5}$ s. The signal length was 219. Fig. 2 shows a fragment of the signal with the duration of 1.4 s.

The vibration signal of a damaged bearing is a carrier signal with a frequency content that depends on the resonant frequencies of the bearing and a modulation signal that is subject to periodic pulses due to the damage. These impulses are not completely periodic due to the random sliding of the rolling elements. In view of this, signals from the carrier frequencies should be demodulated to study the spectral content of the modulation signal, i.e., to detect the influence of impulses. This process involves separating high frequencies from low frequencies by analyzing the envelope vibration to identify the spectral content of the modulation frequencies and then comparing them with the bearing fault frequencies corresponding to faults of bearing elements, which are calculated by the expressions [15, 16]:

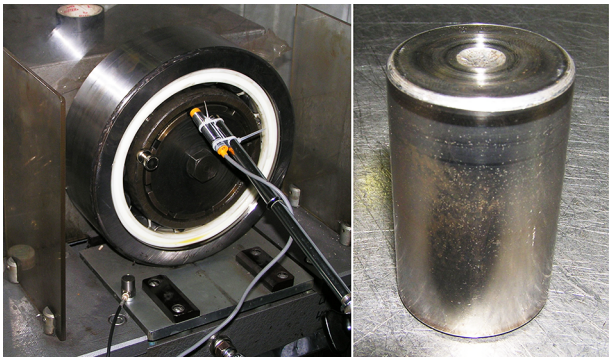

Fig. 1. The damaged bearing on the test rig

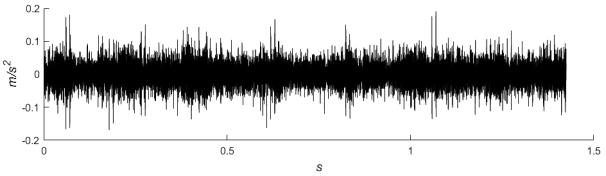

Fig. 2. Wave form of the signal of the damaged bearing

- fundamental train frequency, Hz

$$f_{cg} = \frac{f_r}{2}\left(1 - \frac{d_{rol}}{d_{cg}}\cos\phi\right),$$

where $f_r = n/60 = 12.25$ is shaft speed, Hz; $d_{rol} = 32$ – the roller diameter, mm; $d_{cg} = 190$ – the cage diameter, mm; $\phi = 0$ – an angle of the load from the radial plane, degree;

- roller pass frequency, outer race, Hz

$$f_{outer} = \frac{f_r z}{2}\left(1 - \frac{d_{rol}}{d_{cg}}\cos\phi\right),$$

where $z = 15$ is the number of rollers in the bearing, pcs.;

- roller pass frequency, inner race, Hz

$$f_{inner} = \frac{f_r z}{2}\left(1 + \frac{d_{rol}}{d_{cg}}\cos\phi\right);$$

- roller spin frequency, Hz

$$f_{rol} = \frac{d_{cg} f_r}{2 d_{rol}}\left[1 - \left(\frac{d_{rol}}{d_{cg}}\right)^2 (\cos\phi)^2\right].$$

The calculated values are given in Table 1.

The resonant frequency acts as an information carrier in the amplitude modulated signal. The constructed broadband vibration spectrum can have many resonant frequencies, which require an intuitive approach to selecting exactly the band in which the disturbance is caused by a fault and there is a need for further demodulation to obtain the vibration envelope in this band (Fig. 3) [17].

The envelope can be obtained using the Hilbert transform, which changes the phase of the components by $\pi/2$. The analytical signal has the form

Table 1

Bearing fault frequencies

f_{cg}	f_{outer}	f_{inner}	f_{rol}
5.09 Hz	76.4 Hz	107.35 Hz	35.34 Hz

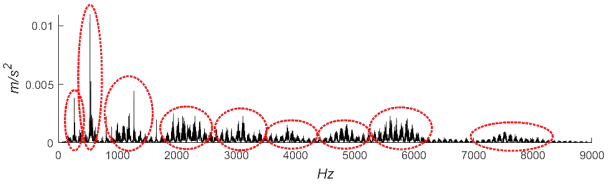

Fig. 3. Broadband vibration spectrum of a bearing with a faulty roller

$$s_a(t) = s(t) + iH(s(t)),$$

where $s(t)$ is time waveform; i – imaginary unit; $H(\ )$ – Hilbert transform of the time waveform [18].

Since determining the informative resonance frequency of a bearing is a challenge [17], to overcome the shortcomings inherent in the intuitive approach to selecting this band, the Fast kurtogram [19] was used, which, according to the highest kurtosis value, calculated the corresponding frequency band of 7.2–7.5 kHz with a central frequency of 7,350 Hz for further construction of the envelope spectrum (Fig. 4).

As noted by Smith and Randall [16], roller faults are the most difficult to detect. The presence of such faults is evidenced by a number of diagnostic features that appear in the envelope spectra, in particular, the frol harmonics, which are surrounded by modulating sidebands at a distance of f_{cg}, as well as the f_{cg} harmonics. Fig. 4 shows 5 f_{cg} harmonics and three f_{rol} harmonics. No modulating sidebands in the vicinity of f_{rol} were detected. It is known [18] that the envelope spectrum can generate spurious higher-order harmonics due to the problem of aliasing, which cannot be avoided.

The squared envelope can prevent aliasing. However, squaring real signals unconditionally implements additional components through aliasing effects. The vibration squared envelope can also be obtained by multiplying the analytical signal by its complex conjugate

$$s_{se}(t) = s_a(t)s_a^*(t).$$

The squared envelope does not involve additional components, but only the desired diagnostic information. Accordingly, the squared envelop is often an effective method to characterize cyclostationary signals. Extracting the squared envelope always includes the noise impact, which fills the vibration signals during vibrodiagnosis and which affects the demodulation accuracy [18]. The constructed squared envelope spectrum (Fig. 5) makes it difficult to find diagnostic features due to the significant noise impact. The features include the first and third f_{cg} harmonics, five f_{rol} harmonics, and a modulating sideband in the vicinity of the third f_{rol} harmonic.

Thus, neither the envelope spectrum nor its more advanced version of the squared envelope spectrum is capable of detecting the entire list of features of roller faults. Therefore, there is a need to develop methods that pre-process the initial signal in order to eliminate noise and increase the number of diagnostic features in the squared envelope spectrum.

The EMD and its junior versions are noteworthy, in particular, EEMD involves white noise to help separate heterogeneous time scales and improve the decomposition efficiency as compared to EMD. The final results of the method are en-

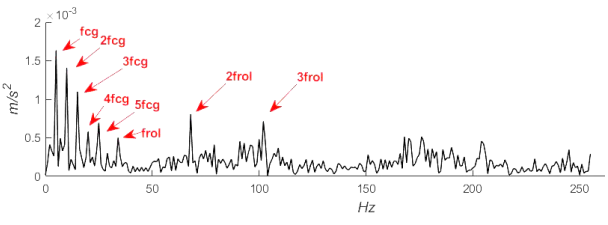

Fig. 4. Envelope vibration spectrum obtained in 7.2–7.5 kHz range

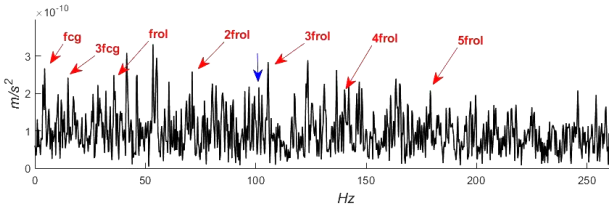

Fig. 5. Squared envelope spectrum obtained within the range of 7.2–7.5 kHz

semble means that are chosen to minimise the effect caused by the additive white noise. With the suggestion of adding white noise to the signal being analyzed, EEMD can be used as a nonlinear and adaptive filter that can extract weak periodic and quasi-periodic signals from noisy signals, especially bearing signals with heavy noise. The main improvement of the EEMD is solving the problem of mode mixing, as it was in EMD, which was known for oscillation of disparate scales. This indicates that the EMD is very sensitive to noise or oscillations [10].

Colominas, et al. [20] proposed an optimized EEMD algorithm that, compared to the classical EEMD, requires less than half the iterations to obtain all IMFs. The main idea of the new tool is to add some noise at each stage of the decomposition and calculate a unique residue to obtain each mode. Compared to EEMD, CEEMDAN has a better ability to extract the impulse trains from the signals generated by faulty bearings.

The improved CEEMDAN does not use white noise directly, but uses the $E_k(\omega^i)$ operator to extract the kth mode. The $M(\cdot)$ operator calculates the local mean of the signal under study, while $\langle\cdot\rangle$ means an averaging action. In EEMD and CEEMDAN, the first mode is determined as follows

$$IMF_1 = \langle x^i\rangle - \langle M(x^i)\rangle.$$

Estimating only the local mean and subtracting it from the initial signal

$$IMF_1 = x - \langle M(x^i)\rangle.$$

ICEEMDAN is implemented by the steps as follows:

Step 1. Implementing EMD to calculate local mean in implementation of $x^i = x + \varepsilon_0 E_1(\omega^i)$, where $i = 1, 2, ..., I$ and obtaining the first residue

$$r_1 = \langle M(x^i)\rangle.$$

Generating $x^i = x + \varepsilon\omega^i$, where ω^i $(i = 1, ..., I)$ implementing white noise with a zero average and unit dispersion rms noise deviation $\varepsilon > 0$.

Step 2. Calculating the first mode $(k = 1)$: $IMF_1 = x - r_1$.

Step 3. Calculating the second residue by averaging local mean implementations of $r_1 + \varepsilon_1 E_2(\omega^i)$ and determining the second mode as

$$IMF_2 = r_1 - r_2 = r_1 - \langle M(r_1 + \varepsilon_1 E_2(\omega^i))\rangle.$$

Step 4. Calculating the k^{th} residue

$$r_k = \langle M(r_{k-1} + \varepsilon_{k-1} E_k(\omega^i))\rangle,$$

where $k = 3, ..., K$.

Step 5. Calculating the k^{th} mode

$$IMF_k = r_{k-1} - r_k.$$

Step 6. Returning to *Step 4* for the next k [20, 21].

The recorded vibration signal was decomposed during the experimental studies using for methods:

1) EMD at 16 IMFs;
2) EEMD at 16 IMFs;
3) CEEMDAN at 19 IMFs;
4) ICEEMDAN at 17 IMFs.

With an increase in the sequence number of each subsequent IMF obtained as a result of the implementation of all

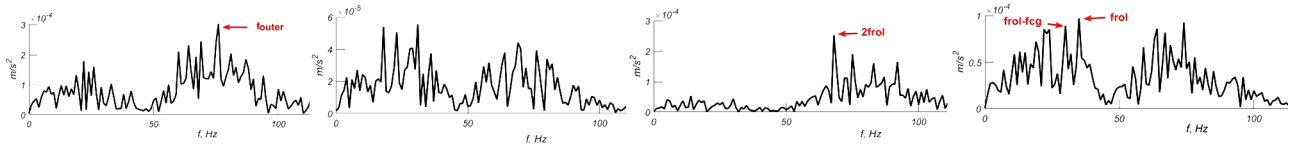

Fig. 6. Vibration FFT spectra of selected IMFs after decomposition using four methods:
a – 8IMF spectrum after EMD; b – 9IMF spectrum after EEMD; c – 12IMF spectrum after CEEMDAN; d – 10IMF spectrum after ICEEMDAN

four methods, the spectra show a shift of energy bursts towards lower frequencies. To search for features of rolling bearing fault, those IMFs were selected whose resonant bursts covered the low-frequency band in accordance with the calculated frequencies in Table 1 (Fig. 6) [22]. The rest of the IMFs were rejected as they had no physical significance. The spectrum of the eighth IMF after decomposition using EMD (Fig. 6, *a*) contains a clearly defined f_{outer} frequency. The spectrum of the ninth IMF after the implementation of the EEMD method (Fig. 6, *b*) does not contain diagnostic features, since it is difficult for EEMD to extract informative components generated by damaged rolling bearing elements. This is due to the fact that the EEMD is based on the EMD method, which in turn is based on the existence of extremes in the signal. Filling the signal with noise prevents EEMD from obtaining an informative signal from noise [10]. The spectrum of the twelfth IMF after the implementation of the CEEMDAN method (Fig. 6, *c*) contains the second f_{rol} harmonic. The spectrum of the tenth IMF after the implementation of the ICEEMDAN method contains the frequency f_{rol} and the left sideband at a distance of f_{cg} (Fig. 6, *d*).

Thus, none of the four methods was able to provide the entire list of features inherent in the fault of the roller on the spectra constructed using the traditional Fast Fourier Transform algorithm and are filled with noise. The largest number of features is shown in the spectrum obtained after the implementation of ICEEMDAN. Once again, the low ability of broadband vibration spectra to detect diagnostic features due to the existing modulation is proved.

In the article, a hybrid vibrodiagnosis method is proposed which decomposes the recoded vibration signal into a number of IMFs using the ICEEMDAN algorithms, selects the most informative IMF with further enhancement of its pulse components using the OMEDA method. Finally, the squared envelope spectrum is used to identify a list of diagnostic features of fault of the rolling bearing elements (Fig. 7).

The IMFs obtained as a result of the decomposition are filled with a high-frequency component at the initial levels of the decomposition. Taking into account the linkage of diagnostic features of the condition of rolling bearings to the shaft speed, at different stages of the study, demodulation and construction of squared envelope spectra were carried out to search for informative frequencies (Table 1).

It has been established that the most common statistical indicator for determining an acceptable IMF is the correlation coefficient (CC) of the obtained modes and the initial vibration implementation. Higher CC values correspond to greater similarity between the mode and the initial signal and, accordingly, a higher probability of the presence of informative components in the mode. However, this indicator is unstable and can demonstrate high or low sensitivity to noise, which causes loss of information, especially when determining the condition of a rolling bearing at the early stages of development, when diagnostic features are difficult to detect in a weak signal with a large amount of noise. Therefore, other indicators are used to prevent the wrong choice of IMF (kurtosis (Kurt), root mean square (RMS)).

The calculation of Kurt alone to extract diagnostic information is also considered ineffective due to the inability to provide an increasing trend of eigenvalues during long-term monitoring of rolling bearings with gradual development of faults. However, the high sensitivity of Kurt to impulsive components in the recorded signals due to initial or developed damage is undeniable. RMS is not effective for detecting a fault that is at an early stage of development.

Since the above indicators are characterized by different diagnostic capabilities to detect the stages of fault development, to determine the informative IMF, the comprehensive evaluation index (CEI) proposed by Gao, et al. [23] was calculated in the article that should decrease the probability of incorrect selection of IMF. The calculated CC of the ten IMFs after decomposition by the ICEEMDAN algorithm formed a range of values from 0.399–0.01 (Table 2). It is worth noting that the CC for the second, third and fourth IMFs was 0.625, 0.626, 0.49. From the fifth to the tenth IMF, a decreasing pattern was clearly observed down to 0.01. The calculated Kurt of the first IMF reached the highest value of 125.18, while the values for the other IMFs were randomly distributed in the range from 2.34 to 6.39. The calculated RMS was in a decreasing range from $4.8 \cdot 10^{-2}$ to $3.3 \cdot 10^{-4}$ m/s^2.

CEI was calculated as the average of the three indicators and ranged from 41.88 for the first IMF to 0.78 for the tenth IMF. It was found that the CEI for the first IMF is eighteen times higher than the highest value for the third IMF, which clearly identifies the first IMF as the most significant one, which can be used for further demodulation and search for informative spectral components that correspond to the rolling frequencies of rollers. The use of CEI eliminates the disadvantages associated with the loss of informative characteristics in IMF due to the use of individual indicators.

Similar calculations were carried out to select the most informative IMF after decomposition using EMD, EEMD, CEEMDAN. CEI was the highest for all three of the first IMFs. The time waveform of the 1IMF signal after EMD is filled with noise the most, while the time waveform after ICEEMDAN contains the least noise among the others.

The time waveforms of the first four IMFs were converted by the fast Fourier transform algorithm into broadband vibration spectra. All four FFT spectra are almost identical, except for the FFT spectrum of the 1st IMF after EMD, where stronger bursts in the range of 3.0–3.5 and 4.5–5.0 kHz are visually noticeable. The fast kurtogram method calculated the highest

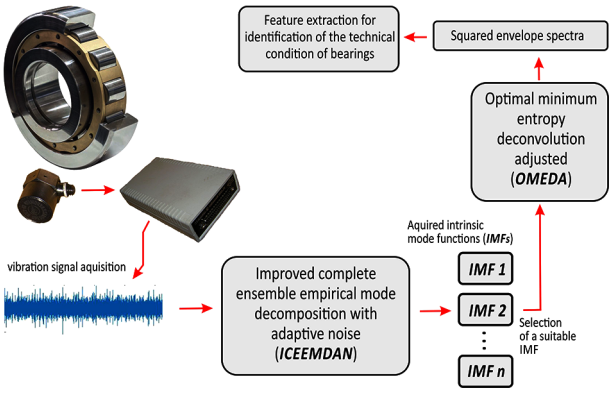

Fig. 7. The proposed hybrid method of roller bearing vibrodiagnosis

Table 2

Calculation of statistical indicators of IMFs

	Kurt	CC	RMS	Average
IMF1	125.18	0.399	$4.8 \cdot 10^{-2}$	41.88
IMF2	5.33	0.625	$9.2 \cdot 10^{-3}$	1.98
IMF3	6.39	0.626	$8.7 \cdot 10^{-3}$	2.34
IMF4	3.74	0.492	$5.5 \cdot 10^{-3}$	1.41
IMF5	3.94	0.381	$5.3 \cdot 10^{-3}$	1.44
IMF6	2.83	0.363	$6.4 \cdot 10^{-3}$	1.07
IMF7	4.36	0.055	$1.2 \cdot 10^{-3}$	1.47
IMF8	2.91	0.02	$6.4 \cdot 10^{-4}$	0.98
IMF9	2.69	0.015	$3.7 \cdot 10^{-4}$	0.9
IMF10	2.34	0.01	$3.3 \cdot 10^{-4}$	0.78

kurtosis in the range of 7.2–7.5 kHz, which was selected for further extraction of the squared envelope spectra (Fig. 8).

All squared envelope spectra are filled with sharp peaks of the f_{rol} harmonics (up to the seventh inclusive) and three f_{cg} harmonics. Thus, the squared envelope spectra after applying the EMD method and its later versions allowed to increase the number of f_{rol} harmonics compared to the squared envelope spectrum in Fig. 4, which was obtained from the initial vibration implementation. Also, unilateral sidebands appeared at the distance f_{cg} from $3f_{rol}$–$5f_{rol}$ (Fig. 8, *a*) and, starting from Figs. 8, *b*, *c*, bilateral sidebands appear around in the vicinity of $4f_{rol}$ and additionally in the vicinity of $5f_{rol}$ (Fig. 8, *d*). All four spectra are also filled with residual noise between the f_{rol} harmonics and in the range above 250 Hz.

Thus, the use of EMD and its later versions provides an increase in diagnostic features on the squared envelope spectra compared to the features on a similar spectrum obtained without pre-processing the recorded vibration signal. However, the significant residual noise requires the use of additional tools to increase the diagnostic features on the squared envelope spectra.

It is known [24] that the kurtosis has gained popularity not only as a diagnostic feature of the condition and as a criterion for selecting an informative vibration frequency band, but also influenced the development and practical application of blind deconvolution methods. The purpose of the blind deconvolution methods, in particular MED, is to iteratively obtain an inverse filter, which changes the convolution process by optimizing the designed objective function. The objective function is generally a mathematical description of the pulse features that directly affect the implementation of the inverse filter.

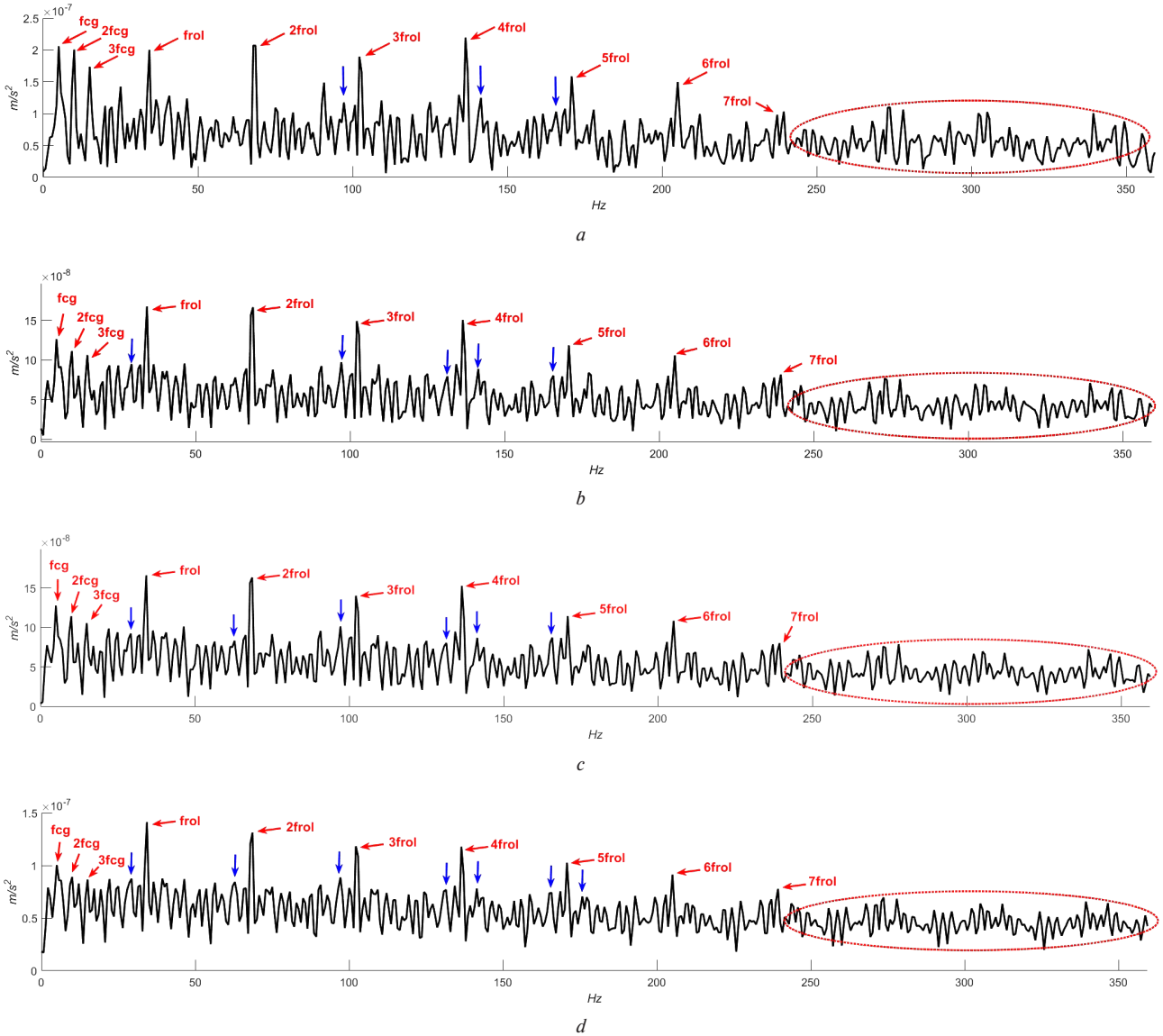

Fig. 8. Squared envelope spectra selected within the range of 7.2–7.5 kHz after the decomposition using the methods below: a – EMD; b – EEMD; c – CEEMDAN; d – ICEEMDAN

Unfortunately, the kurtosis cannot distinguish random pulses from cyclic ones, so MED is not tolerant to noise and often approaches the largest peak in an attempt to extract bursts that are present in the signal. The D-norm is an extended version of the kurtosis that can be used as an objective function to obtain an optimal inverse filter. Similar to kurtosis, the D-norm tends to over-amplify the dominant peaks in the signal. According to the analysis, the choice of the objective function directly affects the efficiency of the inverse filter implementation. Therefore, the first important step in the deconvolution methods is to define the objective function [25].

In this paper, we chose the optimal minimum empirical deconvolution adjusted (OMEDA) method, which was proposed for impulse deconvolution by maximizing the D-norm of the filtered signal [26]. The problem of D-norm deconvolution has an exact non-iterative solution for the filter coefficients.

D-norm of the filtered signal has the form

$$K(f) = \max_{k=1,2,\ldots,N} \frac{|y_k|}{\|y\|},$$

where y is a signal after the inverse filter; $\|y\|$ – Euclidian norm of the signal.

The optimal OMEDA solution is obtaining a filter which tends to maximize the D-norm of the input signal

$$f_{opt} = \{f_{opt}: K(f_{opt}) \geq K(f), \forall f \in \Re^L\}.$$

The optimal OMEDA solution is maximizing the expression for $K(f)$

$$M = (X_0 X_0^T)^- X_0,$$

which corresponds to the fact that the filtered signal has the maximum D-norm. According to the definition of the D-norm, the OMEDA solution is tending to deconvolution single pulses, so OMEDA is sensitive to random pulses [27].

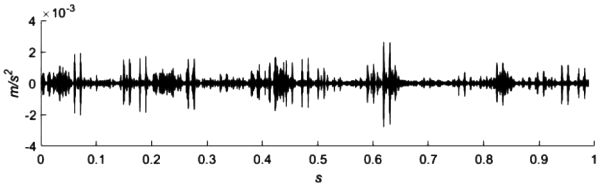

Fig. 9. Time waveform vibration after implementation of the ICEEMDAN + OMEDA hybrid method

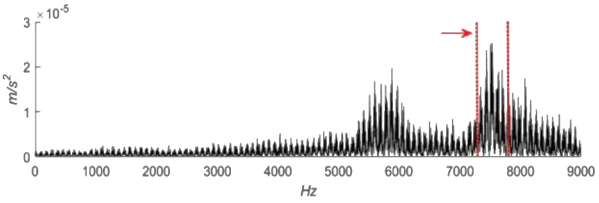

Fig. 10. FFT vibration spectrum after implementation of the ICEEMDAN + OMEDA hybrid method

The further deconvolution of the first IMFs after the implementation of EMD, EEMD, CEEMDAN, and ICEEMDAN was carried out using OMEDA with a filter size of $L = 5$. Fig. 9 shows the time waveform after applying the proposed hybrid ICEEMDAN + OMEDA method. Compared to the 1IMF vibration time waveform after ICEEMDAN, a high-frequency vibration appeared in Fig. 9, a high-frequency component appeared that fills the entire time band of the signal. Fig. 10 shows the corresponding FFT spectrum with a signifi-

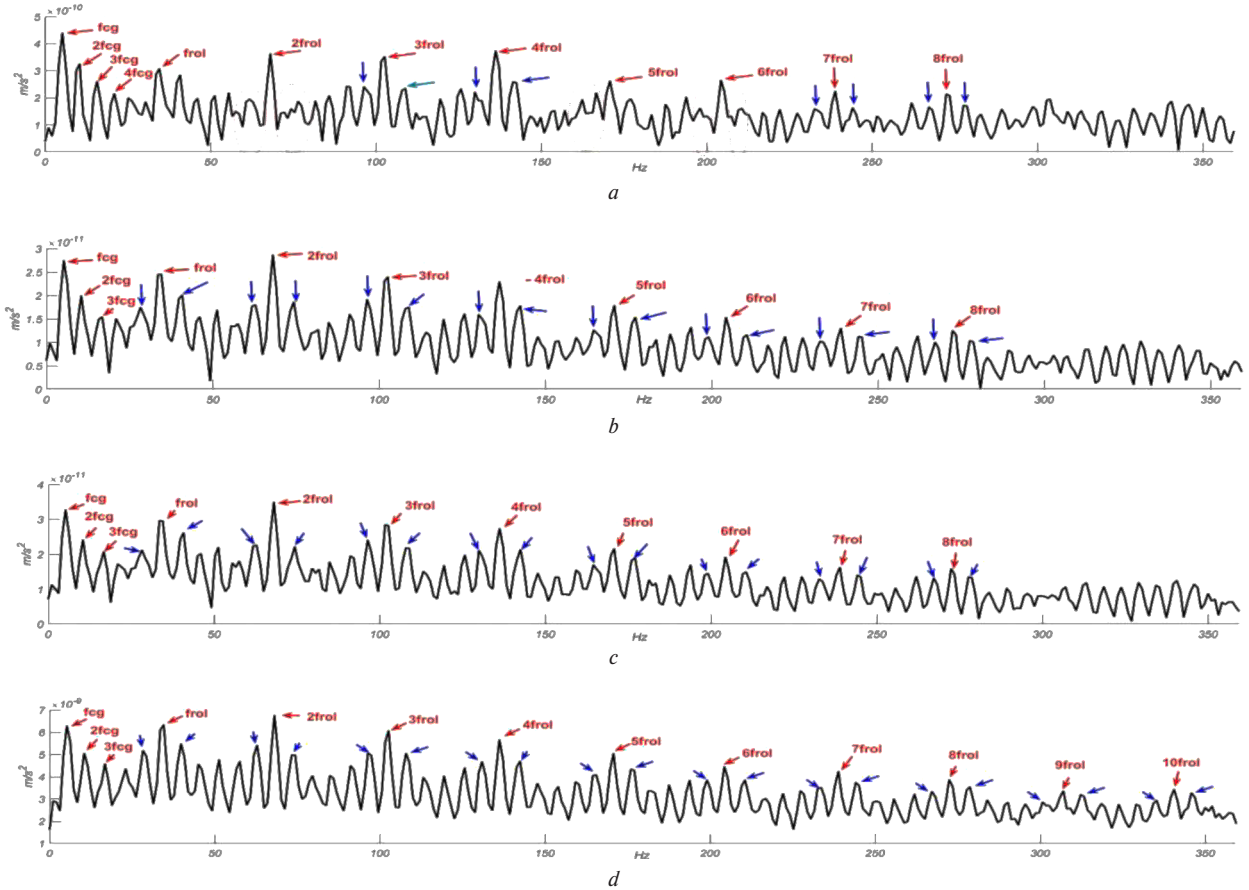

Fig. 11. Squared envelope spectra selected within the band 7.2–7.5 kHz after decomposition using the methods below: a – EMD + OMEDA; b – EEMD + OMEDA; c – CEEMDAN + OMEDA; d – ICEEMDAN + OMEDA

cant energy increase in the range of 7.2–7.5 kHz, which indicates the enhancement of the informative components as a result of the deconvolution using OMEDA.

To compare the effectiveness in the selection of diagnostic features, Fig. 11 shows four squared envelope spectra after additional deconvolution using the OMEDA. The squared envelope spectrum after the 1IMF deconvolution according to the EMD results (Fig. 11, *a*) provided an additional eighth harmonic f_{rol} and caused the appearance of four groups of bilateral sidebands around $3f_{rol}$, $4f_{rol}$, $7f_{rol}$, $8f_{rol}$, in contrast to the results shown in Fig. 8, *a*. The remaining three squared envelope spectra (Figs. 11, *b–d*) contain bilateral sidebands around the frequency f_{rol} and each of its harmonics. Slight residual noise is present only in the vicinity of $2f_{rol}$, $5f_{rol}$ and $6f_{rol}$ (Fig. 11, *a*), while the other three squared envelope spectra do not have any strongly pronounced noise components at all. The largest number of f_{rol} harmonics is presented in Fig. 11, *d*, which determines the combination of ICEEMDAN + OMEDA as the most informative for identifying diagnostic features of the technical condition of bearing rollers in the proposed hybrid method.

Conclusions.

1. Conventional spectral methods for rolling bearing fault vibration diagnosis require mostly intuitive selection of an informative frequency band in the FFT spectrum for further demodulation, which is associated with the probability of selecting a wrong band. Unfortunately, the envelope and squared envelope spectra could only identify a part of the diagnostic features of an axle bearing roller fault, which necessitated the development of a hybrid method for preliminary amplification of informative components in the time waveform of the recorded vibration signals.

2. The approach to selecting an informative IMF after the decomposition procedures was based on the ability of statistical indicators to detect impulse components that should be associated with the existing faults. The kurtosis, correlation coefficient, and RMS value were taken into account by a complex evaluation index, the average value of which was the highest for the first IMFs based on the results of decomposition by EMD, EEMD, CEEMDAN, and ICEEMDAN.

3. The results of decomposition by the EMD and its three versions showed the presence of excessive residual noise in the squared envelope spectra. The largest number of diagnostic features of roller faults, in particular, bilateral side bands, were obtained after using ICEEMDAN.

4. The proposed hybrid method for vibration rolling bearing diagnosis using ICEEMDAN provides an increase in the number of harmonics of roller spin frequencies on the squared envelope spectra, while the OMEDA has enhanced random impulse components in the range of 7.2–7.5 kHz, which resulted in the elimination of residual noise in the squared envelope spectra and the appearance of bilateral sidebands around each harmonic of the roller spin frequencies, providing all the diagnostic features for this type of fault.

References.

1. Wang, Y-Z., Qin, Y., Zhao, X.-J., Zhang, S.-J., & Cheng, X.-Q. (2020). Bearing fault diagnosis with impulsive noise based on EMD and cyclic correntropy. *Proceedings of the 9th International Conference on Green Intelligent Transportation Systems and Safety*. https://doi.org/10.1007/978-981-15-0644-4_112.

2. Rihi, A., Baïna, S., Mhada, F.-z., Elbachari, E., Tagemouati, H., Guerboub, M., & Benzakour, I. (2022). Predictive maintenance in mining industry: grinding mill case study. *Procedia Computer Science, 207*, 2483-2492. https://doi.org/10.1016/j.procs.2022.09.306.

3. Qin, Y., & Jia, L. (2019). *Active safety methodologies of rail transportation. Advances in high-speed rail technology*. Singapore: Springer. ISBN: 978-981-13-2259-4. https://doi.org/10.1007/978-981-13-2260-0.

4. An, G., Tong, Q., Zhang, Y., Liu, R., Li, W., Cao, J., ..., & Pu, X. (2021). A Parameter-Optimized Variational Mode Decomposition Investigation for Fault Feature Extraction of Rolling Element Bearings. *Mathematical Problems in Engineering,* 2021, 6629474. https://doi.org/10.1155/2021/6629474.

5. Dybała, J., & Gałęzia, A. (2014). A Novel Method of Gearbox Health Vibration Monitoring Using Empirical Mode Decomposition. *Proceedings of the Third International Conference on Condition Monitoring of Machinery in Non-Stationary Operations CMMNO 2013*. https://doi.org/10.1007/978-3-642-39348-8_19.

6. Tarek, K., Abderrazek, D., Khemissi, B. M., Cherif, D. M., Lilia, C., & Nouredine, O. (2020). Comparative study between cyclostationary analysis, EMD, and CEEMDAN for the vibratory diagnosis of rotating machines in industrial environment. *The International Journal of Advanced Manufacturing Technology, 109*(9-12), 2747-2775. https://doi.org/10.1007/s00170-020-05848-z.

7. Cheng, J., Yang, Y., Li, X., & Cheng, J. (2021). Adaptive periodic mode decomposition and its application in rolling bearing fault diagnosis. *Mechanical Systems and Signal Processing, 161*, 107943. https://doi.org/10.1016/j.ymssp.2021.107943.

8. Zhang, X., Zhao, J., Ni, X., Sun, F., & Ge, H. (2019). Fault diagnosis for gearbox based on EMD-MOMEDA. *International Journal of System Assurance Engineering and Management, 10*(4), 836-847. https://doi.org/10.1007/s13198-019-00818-5.

9. Li, H., Liu, T., Wu, X., & Chen, Q. (2019). Application of EEMD and improved frequency band entropy in bearing fault feature extraction. *ISA Transactions, 88*, 170-185. https://doi.org/10.1016/j.isatra.2018.12.002.

10. Guo, W., Tse, P. W., & Djordjevich, A. (2012). Faulty bearing signal recovery from large noise using a hybrid method based on spectral kurtosis and ensemble empirical mode decomposition. *Measurement, 45*(5), 1308-1322. https://doi.org/10.1016/j.measurement.2012.01.001.

11. Kedadouche, M., Thomas, M., & Tahan, A. (2014). Monitoring Machines by Using a Hybrid Method Combining MED, EMD, and TKEO. *Advances in Acoustics and Vibration, 2014*, 1-10. https://doi.org/10.1155/2014/592080.

12. Ahn, J.-H., Kwak, D.-H., & Koh, B.-H. (2014). Fault Detection of a Roller-Bearing System through the EMD of a Wavelet Denoised Signal. *Sensors, 14*(8), 15022-15038. https://doi.org/10.3390/s140815022.

13. Bouhalais, M. L., Djebala, A., Ouelaa, N., & Babouri, M. K. (2018). CEEMDAN and OWMRA as a hybrid method for rolling bearing fault diagnosis under variable speed. *The International Journal of Advanced Manufacturing Technology, 94*(5-8), 2475-2489. https://doi.org/10.1007/s00170-017-1044-0.

14. He, C., Niu, P., Yang, R., Wang, C., Li, Z., & Li, H. (2019). Incipient rolling element bearing weak fault feature extraction based on adaptive second-order stochastic resonance incorporated by mode decomposition. *Measurement, 145*, 687-701. https://doi.org/10.1016/j.measurement.2019.05.052.

15. Saidi, L., Ali, J. B., Benbouzid, M., & Bechhoefer, E. (2016). The use of SESK as a trend parameter for localized bearing fault diagnosis in induction machines. *ISA Transactions, 63*, 436-447. https://doi.org/10.1016/j.isatra.2016.02.019.

16. Smith, W. A., & Randall, R. B. (2015). Rolling element bearing diagnostics using the Case Western Reserve University data: A benchmark study. *Mechanical Systems and Signal Processing, 64-65*, 100-131. https://doi.org/10.1016/j.ymssp.2015.04.021.

17. Klausen, A., Robbersmyr, K. G., & Karimi, H. R. (2017). Autonomous Bearing Fault Diagnosis Method based on Envelope Spectrum. *IFAC-PapersOnLine, 50*(1), 13378-13383. https://doi.org/10.1016/j.ifacol.2017.08.2262.

18. Xu, Y., Feng, G., Tang, X., Yang, S., Fengshou, G., & Ball, A. D. (2023). A Modulation Signal Bispectrum Enhanced Squared Envelope for the detection and diagnosis of compound epicyclic gear faults. *Structural Health Monitoring, 22*(1), 562-580. https://doi.org/10.1177/14759217221098577.

19. Randall, R. B. (2021). *Vibration-based condition monitoring*. NJ: John Wiley & Sons Ltd. ISBN: 978-1-119-47755-6.

20. Colominas, M. A., Schlotthauer, G., & Torres, M. E. (2014). Improved complete ensemble EMD: A suitable tool for biomedical signal processing. *Biomedical Signal Processing and Control, 14*, 19-29. https://doi.org/10.1016/j.bspc.2014.06.009.

21. Rabah, A., & Abdelhafid, K. (2018). Rolling bearing fault diagnosis based on improved complete ensemble empirical mode of decomposition with adaptive noise combined with minimum entropy deconvol ution. *Journal of Vibroengineering, 20*(1), 240-257. https://doi.org/10.21595/jve.2017.18762.

22. Lei, Y., Liu, Z., Ouazri, J., & Lin, J. (2017). A fault diagnosis method of rolling element bearings based on CEEMDAN. *Proceedings of the Institution of Mechanical Engineers, Part C: Journal of Me-*

chanical Engineering Science, 231(10), 1804-1815. https://doi.org/10.1177/0954406215624126.
23. Gao, K., Xu, X., Li, J., Jiao, S., & Shi, N. (2021). Application of multi-layer denoising based on ensemble empirical mode decomposition in extraction of fault feature of rotating machinery. *PLoS ONE, 16*(7), e0254747. https://doi.org/10.1371/journal.pone.0254747.
24. Miao, Y., Zhang, B., Lin, J., Zhao, M., Liu, H., Liu, Z., & Li, H. (2022). A review on the application of blind deconvolution in machinery fault diagnosis. *Mechanical Systems and Signal Processing, 163*, 108202. https://doi.org/10.1016/j.ymssp.2021.108202.
25. He, L., Yi, C., Wang, D., Wang, F., & Lin, J.-h. (2021). Optimized minimum generalized Lp/Lq deconvolution for recovering repetitive impacts from a vibration mixture. *Measurement, 168*, 108329. https://doi.org/10.1016/j.measurement.2020.108329.
26. McDonald, G.L., & Zhao, Q. (2017). Multipoint Optimal Minimum Entropy Deconvolution and Convolution Fix: Application to vibration fault detection. *Mechanical Systems and Signal Processing, 82*, 461-477. https://doi.org/10.1016/j.ymssp.2016.05.036.
27. Cheng, Y., Wang, Z., Zhang, W., & Huang, G. (2019). Particle swarm optimization algorithm to solve the deconvolution problem for rolling element bearing fault diagnosis. *ISA Transactions, 90*, 244-267. https://doi.org/10.1016/j.isatra.2019.01.012.

Гібридний метод вібродіагностування підшипника кочення рухомого складу з використанням ICEEMDAN та OMEDA

В. Г. Пузир, *С. В. Михалків*[*], *О. А. Плахтій*

Український державний університет залізничного транспорту, м. Харків, Україна
[*] Автор-кореспондент e-mail: svm_m@kart.edu.ua

Мета. Полягає в розробці гібридного методу, що заснований на процедурах ICEEMDAN і OMEDA для визначення діагностичних ознак технічного стану ролика підшипника кочення з високою достовірністю.

Методика. Пошук інформативних частотних компонент на широкосмугових спектрах, спектрах обвідної та квадратичної обвідної вібрації за результатами реалізації методів цифрової обробки сигналів. Використання методів математичної статистики для відбору інформативних IMFs за результатами виконання ітераційних обчислювальних процедур. Залучення методу сліпої розгортки з відповідною цільовою функцією для посилення імпульсних ознак, що викликані пошкодженнями.

Результати. Використання традиційних спектральних методів надало неповний перелік діагностичних ознак, властивих пошкодженню ролика підшипника кочення. Метод розкладання за емпіричними модами (EMD) і його молодші версії надали групи вбудованих функцій мод (IMFs). На широкосмугових спектрах вібрації відібраних низькочастотних IMFs діагностичних ознак у достатній кількості не було виявлено. Подальші дослідження зосередились на розробці гібридного методу, що зважає на процедуру демодуляції високочастотних складових тих IMFs, які відбирались за комплексним індексом оцінювання. Метод швидкої ексцесограми визначив інформативну частотну смугу 7.2–7.5 кГц для демодуляції й побудови квадратичних спектрів обвідної вібрації, де з'явились гармоніки частоти обертання ролика й деякі бічні смуги з шириною, що дорівнює частоті обертання сепаратора. Застосування OMEDA дозволило позбутись на спектрах квадратичної обвідної вібрації залишкового шуму й спричинити появу двосторонніх бічних смуг навколо всіх гармонік частоти обертання роликів.

Наукова новизна. Уперше виявлено весь перелік діагностичних ознак пошкодження ролика підшипника кочення буксового вузла рухомого складу завдяки розробленому гібридному методу, що залучає заходи зі зменшення шуму для набуття фізичного значення певних частотних складових, які пов'язані з пошкодженням. Використання оптимального скоригованого методу розгортки з мінімальною ентропією дозволило остаточно позбутись шуму й надати весь перелік діагностичних ознак технічного стану на квадратичному спектрі обвідної вібрації.

Практична значимість. Результати проведених досліджень дозволять на випробувальному стенді у відділенні з ремонту роликових підшипників вантажного вагонного депо контролювати якість ремонту підшипників буксових вузлів.

Ключові слова: *вагон, вібрація, діагностика, підшипник, розгортка, розкладання, спектр*

The manuscript was submitted 14.09.23.